Changes of Surface Area in the Dissolution Process of Crystalline Substances. IV. Dissolution and Simulation Curves Estimated from Changes of Surface Area and Cube Root Law

Hisakazu SUNADA, Itaru SHINOHARA, Akinobu OTSUKA and Yorinobu YONEZAWA*

Faculty of Pharmacy, Meijo University, Tempaku-cho, Tempaku-ku, Nagoya 468, Japan. *Received November 16, 1988*

The dissolution of *n*-propyl *p*-hydroxybenzoate was conducted under the sink condition, and was simulated from the changes of surface area during the dissolution process and by means of the cube root law. The surface area of the samples was estimated by using a LUZEX image analyzer. The two simulation methods gave almost the same dissolution rate constants.

Dissolution of systems prepared by mixing sieved samples at various weight ratios was also carried out, and these dissolution processes were simulated by means of the cube root law. The apparent mean diameter of the mixed systems was well estimated in terms of particle size and weight ratio of the components. Hence, the mixed systems were converted into several imaginary equivalent systems, and the applicability of the cube root law and the validity of the estimation of apparent mean diameter of the mixed system were examined.

Keywords paraben; *n*-propyl *p*-hydroxybenzoate; crystalline particle; dissolution; surface area; image analyzer; mixed system; imaginary system; simulation; cube root law

Introduction

The dissolution process is an important factor which influences the bioavailability of sparingly soluble drugs. Dissolution behavior of powder or a tablet which easily disintegrates depends on the particle size, and hence, the particle surface area. We have reported the dissolution profiles and their simulation for mixed systems of sieved components on the basis of the changes of surface area during the dissolution process of component samples.[1] We have been treating the dissolution behavior in terms of the changes of surface area with dissolution time. In other words, the treatment is based on the changes of particle size. Hence, there is a similarity in the treatments based on the changes of surface area and the use of the cube root law.

In this paper, the dissolution process of sieved samples was simulated by means of the cube root law, and the method was compared with the simulation method based on the changes of surface area. According to the cube root law equation, the dissolution behavior is defined by the initial particle size for a monodisperse system. Therefore, when the dissolution behavior of a polydisperse system is well defined by the cube root law, an apparent mean particle size might be evaluated. There have been several reports concerning the application of the cube root law to simulate the dissolution behavior of polydisperse systems[2] without employing an apparent mean particle size. Hence, the dissolution behaviors of mixed systems devised to have symmetrical particle size distribution were simulated on the base of the cube root law, and the results are discussed in terms of an apparent mean particle size of the mixed systems.

Experimental

Materials The samples examined in the previous paper were used.[1b,c] *n*-Propyl *p*-hydroxybenzoate (extra pure reagent, Kanto Chemical Co., Ltd.) separated into 14/20, 20/28 and 28/35 mesh fractions by the use of J.I.S. sieves were abbreviated as Pr-PHBA(L), Pr-PHBA(M) and Pr-PHBA(S), respectively; their Heywood's diameter measured by using a LUZEX-500 image analyzer were 0.134, 0.104 and 0.076 cm, respectively. Sieved samples, 35/48 (0.051 cm) and 35/65 (0.048 cm) mesh fractions, were also used.

Dissolution of Crystalline Particles A suitable amount of sieved sample (less than one-twentieth of the solubility) was added to a dissolution apparatus (type NTR-VS, Toyama Sangyo Co., Ltd.) coupled to a flow cell set in a spectrophotometer (type 200-20, Hitachi Ind. Co.) *via* a pump. Following the method described in previous papers,[1b,c] the dissolution measurement was carried out in 1000 ml of water at a paddle rotation speed of 250 rpm at 25 °C. The concentration was estimated from the absorbance at 255 nm.

Sieved samples mixed at various weight ratios were also used for dissolution measurements.

Results and Discussion

Dissolution and Simulation Curves Estimated from Changes of Surface Area and from the Cube Root Law The dissolution rate (dC/dt) given by Nernst[3] is expressed by Eq. 1, where D is the diffusion constant, S the effective surface area and δ the thickness of the diffusion layer.

$$dC/dt=(DS/V\delta)(C_s-C) \quad (1)$$

Here, C_s is the solubility, C is the concentration in the dissolution process and V is the volume of solvent. When the surface area changes with dissolution and C is small enough to consider that the dissolution is carried out under the sink condition, Eq. 1 can be transformed to Eq. 2 by the use of $S(t)$ in place of S.

$$dC/dt=(kC_s/V)S(t) \quad (2)$$

Here, $k=D/\delta$ and is the dissolution rate constant per unit area. Taking account of the coefficient (f)[1b] concerned with shape, which was deduced in connection with Heywood's diameter (D_H), Eq. 3 is derived from Eq. 2:

$$dC=(kC_s/V)n\pi(fD_H)^2dt \quad (3)$$

where n is the number of particles.

On the other hand, the concentration is expressed by Eq. 4 in terms of the initial particle diameter ($D_{H,0}$) and the density (ρ).

$$C=(n\pi\rho/6V)f^3(D_{H,0}^3-D_H^3) \quad (4)$$

Equation 5 is obtained by differentiating Eq. 4, and Eq. 6 is deduced from Eqs. 3 and 5. Then, Eq. 7 is obtained by integrating Eq. 6.

$$dC=-(n\pi\rho f^3/2V)D_H^2dD_H \quad (5)$$

$$-dD_H=(2kC_s/\rho f)dt \quad (6)$$

$$D_{H,\circ} - D_H = (2kC_s/\rho f)t \quad (7)$$

By multiplying by $f(n\pi)^{1/2}$, Eq. 7 is transformed to Eqs. 8 and 9.

$$S(t)_\circ^{1/2} - S(t)^{1/2} = (2kC_s/\rho f)\{S(t)_\circ^{1/2}/D_{H,\circ}\}t \quad (8)$$

$$\{S(t)/S(t)_\circ\}^{1/2} = 1 - (2kC_s/\rho f)(t/D_{H,\circ}) \quad (9)$$

By multiplying by $f(n\pi\rho/6)^{1/3}$, Eq. 7 is transformed to Eq. 10, as Hixson and Crowell deduced,[4] and Eqs. 11 and 12 are obtained.

$$M_\circ^{1/3} - M^{1/3} = (2kC_s/\rho f)(M_\circ^{1/3}/D_{H,\circ})t \quad (10)$$

$$M^{1/3} = M_\circ^{1/3}\{1 - (2kC_s/\rho f)(t/D_{H,\circ})\} \quad (11)$$

$$(M/M_\circ)^{1/3} = 1 - (2kC_s/\rho f)(t/D_{H,\circ}) \quad (12)$$

Here, $M_\circ$ is the amount used and M is the amount remaining in the solution ($=M_\circ - m$, m is the amount dissolved). The values of $D_{H,\circ}$, D_H, $S(t)_\circ$ and $S(t)$ were obtained by using a LUZEX-500 image analyzer,[1b] and the values of $M_\circ$ and M were obtained by dissolution measurements. The applicability of Eq. 9 was examined by the use of the same data which had been used to estimate the k-value from Eq. 2 in the previous paper,[1a] and is shown in Fig. 1. According to Eq. 9, when changes of surface area are treated in terms of $t/D_{H,\circ}$, a single straight line should be obtained independently of the original surface area and particle size. A fairly good straight line was obtained (Fig. 1), and the k-value calculated from the slope and Eq. 9 was 0.171 cm/min, where $C_s = 0.00033$ g/ml, $\rho = 1.28$ g/cm^3 and $f = 0.3690$,[1b] which coincided well with the k-value obtained from Eq. 2, *i.e.*, 0.170 cm/min.[1b]

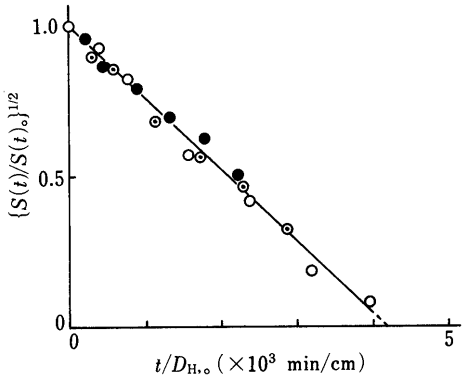

Fig. 1. Applicability of Eq. 9

Amount of Pr-PHBA, 16.4 mg; ●, Pr-PHBA (L); ⊙, Pr-PHBA (M); ○, Pr-PHBA (S).

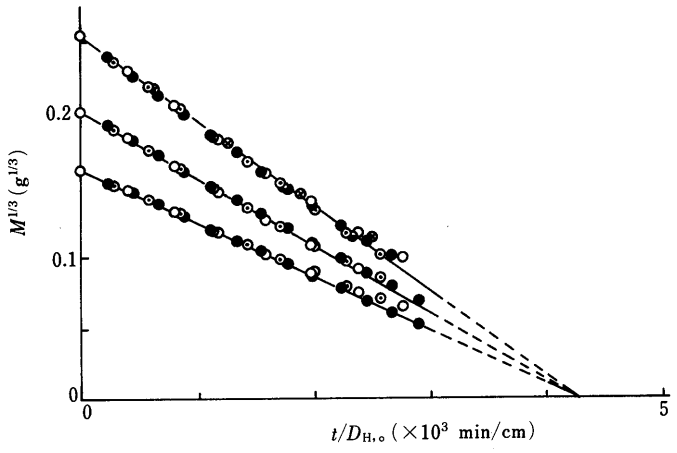

Fig. 2. Applicability of Eq. 11

●, Pr-PHBA (L); ⊙, Pr-PHBA (M); ○, Pr-PHBA (S); ◒, Pr-PHBA (35/48); ⊗, Pr-PHBA (35/65).

The applicability of the cube root law was examined with various initial amounts of sieved samples, and the dissolution results are shown in Figs. 2 and 3. According to Eq. 11, the dissolution of the same amount of different particle samples should be expressed by a single straight line, and the lines obtained from different initial amounts should intersect at one point on the $t/D_{H,\circ}$-axis. The applicability and validity of the treatment can be seen in Fig. 3. The k-value was obtained as 0.166 cm/min, even though dissolution was carried out with different amounts and particle size of samples. Thus the k-value obtained from the cube root law agrees fairly well with the value obtained by the use of the changes of surface area, and hence, the cube root law is considered to be a useful method to simulate dissolution processes.

Simulation and Dissolution Curves for Mixed Systems Estimated from the Cube Root Law In a mixed system, the dissolution process of each component is expressed by Eq. 13 (from Eq. 10), and the total amount and amount remaining in the solution should be given by Eqs. 14 and 15, respectively, as the summation of the components:

$$w_i^{1/3} = w_{i,\circ}^{1/3} - (2kC_s w_{i,\circ}^{1/3}/\rho f)(t/D_{H,i}) \quad (13)$$

$$M_\circ = \sum w_{i,\circ} \quad (14)$$

$$M = \sum w_i \quad (15)$$

where $w_{i,\circ}$ is the amount used, w_i is the amount remaining in the solution and $D_{H,i}$ is the initial Heywood's diameter of component i. Hence, the amount remaining in the solution can be expressed by Eq. 16 following the description for a monodisperse system.[2f,5]

$$M^{1/3} = M_\circ^{1/3} - \sum\{(2kC_s w_{i,\circ}^{1/3}/\rho f)(t/D_{H,i})\} \quad (16)$$

Equation 16 can be transformed to Eqs. 17 and 18:

$$(M/M_\circ)^{1/3} = 1 - (2kC_s/\rho f)\sum\{(w_{i,\circ}/M_\circ)^{1/3}(t/D_{H,i})\} \quad (17)$$

$$(M/M_\circ)^{1/3} = 1 - (2kC_s/\rho f D_v)t \quad (18)$$

where $D_v = \{M_\circ/\sum(w_{i,\circ}/D_{H,i}^3)\}^{1/3}$ and is the mean volume diameter. Thus, the amount remaining in the solution might be expressed by Eq. 18. Another equation, ex-

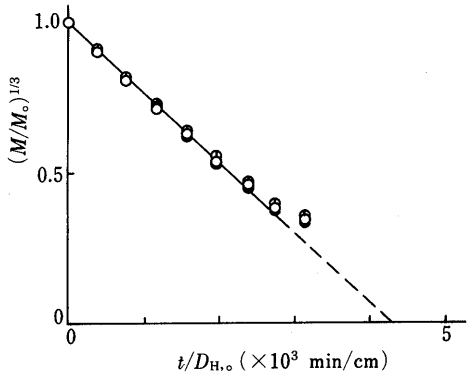

Fig. 3. Applicability of Eq. 12

Amount of Pr-PHBA (S) (mg): ○, 16.4; ●, 8.2; ⓓ, 4.1.

pressed by Eq. 19, was also tried:

$$(M/M_\infty)^{1/3} = 1 - (2kC_s/\rho f D_w)t \quad (19)$$

where $D_w = (\sum w_{i,\infty} D_{H,i})/M_\infty$ and is the volume mean diameter.

The relationship between $(M/M_\infty)^{1/3}$ and t obtained from the dissolution measurement of a mixed system is shown in Fig. 4. There is a good linear relationship, and the apparent mean diameter (D_{app}) of the mixed system can be estimated from the slope. The D_{app}-values obtained by the above method for all the systems are listed in Table I. On the other hand, the D_v-value and the D_w-value were estimated in terms of the particle size and weight of components, and are summarized in Table I. The relationships between the various mean diameters obtained are shown in Fig. 5. Good correlations exist, and the following equations were obtained.

$$D_{app} = 1.090 D_v \quad (20)$$

$$D_{app} = 0.995 D_w \quad (21)$$

According to the equations, the D_w-value is closer to the D_{app}-value than the D_v-value. On the other hand, Fig. 5 shows that the D_v-values deviate from the line less than do the D_w-values, and it appears that Eq. 18 is reasonable. However, the D_{app}-values are well defined by the use of the

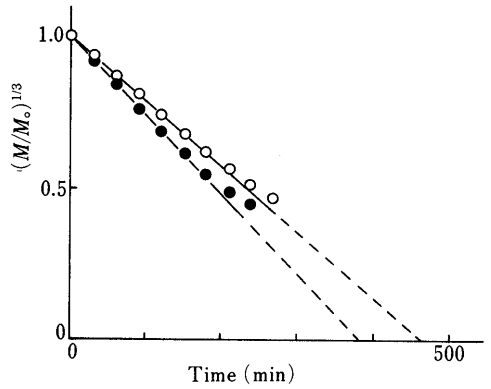

Fig. 4. Applicability of Eq. 12 for the Dissolution of Mixed Systems
○, mixed system II; ●, mixed system V.

TABLE I. Diameters of Mixed Systems

Mixed system	Amount of Pr-PHBA (mg)			Diameter (cm)		
	(S)	(M)	(L)	D_{app}	D_v	D_w
I	2.0	12.4	2.0	0.1066	0.1001	0.1045
II	3.0	10.4	3.0	0.1072	0.0982	0.1045
III	4.0	8.4	4.0	0.1024	0.0964	0.1046
IV	5.0	6.4	5.0	0.1037	0.0948	0.1047
V	11.5	1.6	3.3	0.0887	0.0824	0.0902
VI	10.4	3.0	3.0	0.0885	0.0837	0.0916
VII	4.9	7.8	3.7	0.1050	0.0940	0.1025
VIII	8.2	1.6	6.6	0.0940	0.0892	0.1020
IX	4.0	4.0	8.4	0.1097	0.1003	0.1126
X	2.7	5.5	8.2	0.1156	0.1042	0.1145
XI	3.0	3.0	10.4	0.1151	0.1057	0.1180
XII	1.6	1.6	13.2	0.1307	0.1158	0.1256

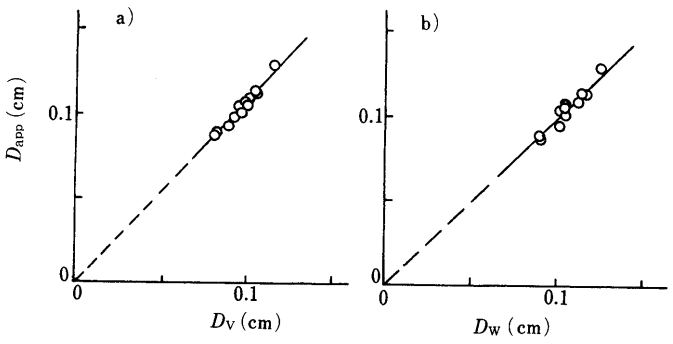

Fig. 5. Relationships between the Mean Diameters
a) Relationship between D_{app} and D_v. b) Relationship between D_{app} fand D_w.

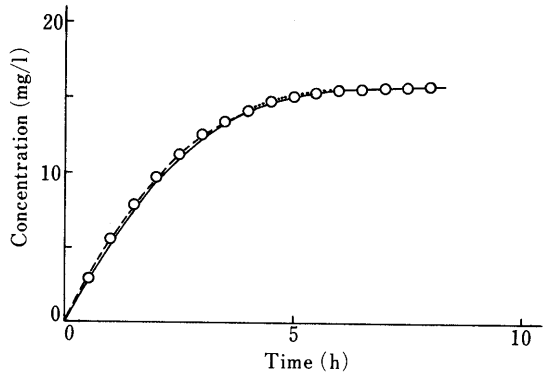

Fig. 6. Simulation Curves for Mixed System II
------, C_T; ——, C_v; ····, C_w.

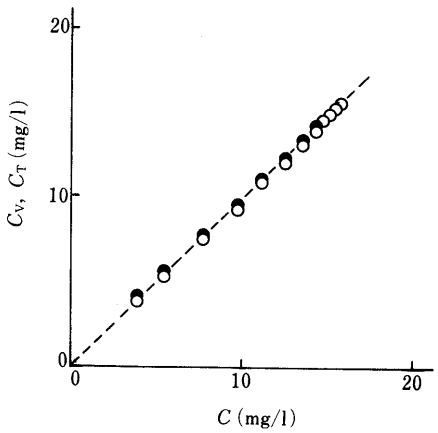

Fig. 7. Relationship between the Simulated Values (C_T, C_v) and the Measured Value (C) for Mixed System II
●, C_T; ○, C_v. ---, C_T and/or C_v equal C.

TABLE II. Evaluation of Simulated Values for Mixed Systems

Mixed system	$\bar{R}_T \pm$S.D.	$\bar{R}_v \pm$S.D.	$\bar{R}_w \pm$S.D.
I	0.993±0.009	0.977±0.024	0.993±0.011
II	0.998±0.005	0.987±0.018	0.997±0.010
III	0.987±0.015	0.980±0.026	0.983±0.023
IV	0.992±0.009	0.991±0.016	0.988±0.018
V	0.989±0.010	0.983±0.024	0.983±0.024
VI	0.987±0.018	0.981±0.030	0.979±0.030
VII	1.001±0.004	0.995±0.014	0.995±0.014
VIII	0.979±0.026	0.984±0.035	0.971±0.046
IX	0.987±0.012	0.991±0.019	0.983±0.026
X	0.998±0.010	0.996±0.013	0.995±0.013
XI	0.978±0.020	0.978±0.025	0.971±0.030
XII	1.006±0.009	1.001±0.009	1.005±0.008

S.D., standard deviations.

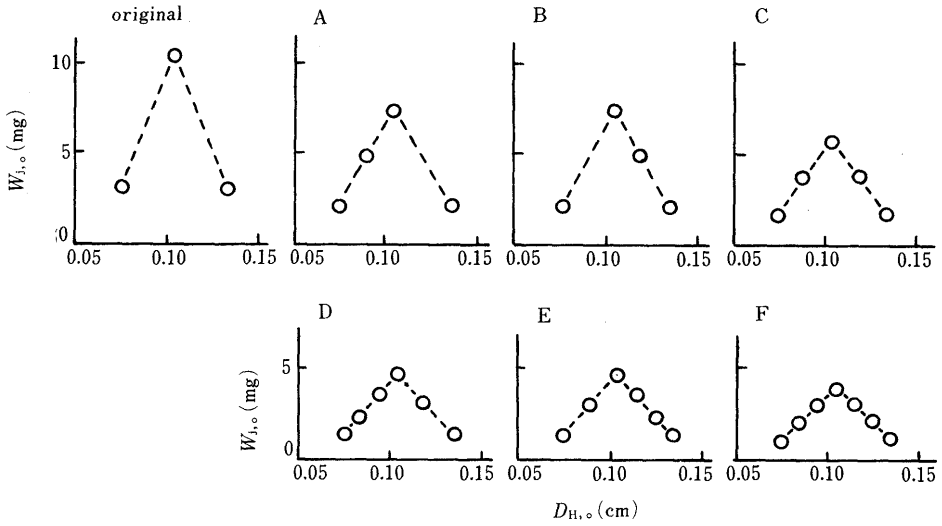

Fig. 8. Original and Imaginary Systems for Mixed System II

D_v- and D_w-values.

Dissolution processes were simulated as follow. The concentrations, *i.e.*, C_T, C_v and C_w, were estimated by the use of Eq. 22 (deduced from Eqs. 13, 14 and 15), Eq. 23 (deduced from Eqs. 18 and 20) and Eq. 24 (deduced from Eqs. 19 and 21), respectively, and the simulation curves of a mixed system are shown in Fig. 6. The simulated values are also shown in Fig. 7 to clarify the correlation with the measured value (C).

$$C_T=(1/V)\sum w_{i,}\,[1-\{1-(2kC_s/\rho f D_{H,i})t\}^3] \quad (22)$$

$$C_v=(M/V)[1-\{1-(2kC_s/1.090\times\rho f D_v)t\}^3] \quad (23)$$

$$C_w=(M/V)[1-\{1-(2kC_s/0.995\times\rho f D_w)t\}^3] \quad (24)$$

The broken line shown in Fig. 7 is the line C_T and/or C_v equal to C. The simulated values are very close to the measured values. Hence, the ratios of simulated value to measured value, *i.e.*, C_T/C ($=R_T$), C_v/C ($=R_v$) and C_w/C ($=R_w$), were used to estimate the validity of the simulation, as described in previous papers,[1b,c] and the mean values of the ratios ($\bar{R}_T$, $\bar{R}_v$ and $\bar{R}_w$) and standard deviations are summarized in Table II. The C_T-value is the highest and the C_v-value is the lowest in the initial stage of dissolution, and the C_w-value is the highest and the C_T-value is the lowest in the middle stage (Fig. 6). However, the values listed in Table II are very close to each other, and are also very close to unity. Therefore, these methods seem to be useful to simulate the dissolution process of mixed systems.

Simulation of Dissolution for Mixed Systems Estimated from Imaginary Particle Size Distributed Systems In the previous section, the apparent mean diameter of a mixed system was well defined by the mean volume diameter and/or the volume mean diameter. As the values of D_v and D_w can be calculated from the particle size and weight of components in the mixed system, the validity and applicability of the methods were examined by simulating the dissolution of a mixed system by means of several imaginary equivalent systems as described in a previous paper.[1c] The samples had been sieved before use, but should still be composed of crystals of various particle sizes, even if in a narrow range. Hence, some imaginary components were chosen as the middle, one-third and two-thirds particle sizes between Pr-PHBA(S) and (M) or Pr-PHBA(M) and (L). The amount of each component was calculated along the broken line of the original mixed system as shown in Fig. 8, even though some deviations from the real particle size distribution in the mixed system might exist. Thus, the three-component system was transformed to systems with four to seven components (types A—F), and the validity and applicability of the simulation methods were examined. Here, the simulation by means of Eq. 22, *i.e.*, C_T, was done in terms of $\bar{R}_T$ and D_T (apparent mean diameter obtained by the use of Eq. 18 and the amounts evaluated from the C_T-values), and that in terms of D_v and

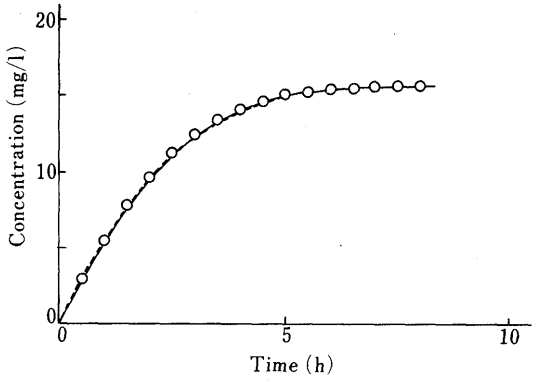

Fig. 9. Simulation Curves (C_T) Evaluated from the Original System and Type F Imaginary System for Mixed System II

---, original system; ——, type F imaginary system.

TABLE III. Evaluation of Simulation with Imaginary Systems

Type	$\bar{R}_T \pm$ S.D.			
	I	II	III	IV
Original	0.993±0.009	0.998±0.005	0.987±0.015	0.992±0.009
A	1.007±0.011	1.010±0.012	0.997±0.008	1.002±0.008
B	0.982±0.020	0.986±0.016	0.975±0.027	0.982±0.019
C	0.994±0.008	0.998±0.005	0.986±0.016	0.992±0.010
D	1.001±0.007	1.005±0.007	0.992±0.011	0.998±0.006
E	0.988±0.014	0.991±0.011	0.979±0.023	0.985±0.017
F	0.994±0.008	0.998±0.005	0.986±0.017	0.991±0.011

TABLE IV. Diameters of Imaginary Systems

Type	D_v (cm)				D_w (cm)				D_T (cm)			
	I	II	III	IV	I	II	III	IV	I	II	III	IV
Original	0.1001	0.0982	0.0964	0.0948	0.1045	0.1045	0.1046	0.1047	0.1047	0.1022	0.1026	0.1015
A	0.0965	0.0955	0.0945	0.0934	0.1000	0.1003	0.1006	0.1009	0.0995	0.1002	0.1002	0.0988
B	0.1046	0.1028	0.1010	0.0992	0.1090	0.1088	0.1086	0.1084	0.1082	0.1075	0.1078	0.1061
C	0.1004	0.0992	0.0981	0.0970	0.1044	0.1046	0.1046	0.1047	0.1033	0.1043	0.1036	0.1029
D	0.0983	0.0974	0.0965	0.0955	0.1022	0.1022	0.1022	0.1022	0.1026	0.1022	0.1015	0.1005
E	0.1027	0.1017	0.1007	0.0996	0.1069	0.1069	0.1070	0.1071	0.1064	0.1061	0.1057	0.1050
F	0.1005	0.0996	0.0987	0.0987	0.1045	0.1046	0.1046	0.1046	0.1050	0.1047	0.1029	0.1029

D_w was done by comparing the value with the D_{app}-value obtained from the dissolution measurement, since the correlation coefficient between the D_{app}-value and the D_v-value or the D_w-value changes with the imaginary system.

A simulation curve obtained is shown in Fig. 9 as an example. The ratio of simulated values to measured values was used to estimate the validity, as described before, and the mean value and standard deviation are summarized in Table III. The D_v-, D_w- and D_T-values are summarized in Table IV. The mean value ($\bar{R}_T$) for all the imaginary systems which deviate only slightly from unity shows that the simulated values coincide well with the measured values and the D_T-values are close to the D_{app}-values. Also, the D_v-values and the D_w-values calculated with the imaginary systems are close to those of the original system, and it appears that the introduction of imaginary particles does not cause any problem in the simulation of the dissolution process. An increase or decrease in mean diameter causes a higher or lower simulation value, respectively. Hence, comparing the simulated values for the imaginary systems with those of the original system, the value become a little higher or lower in accordance with the introduction of imaginary components to emphasis the smaller particle size region (types A and D) or larger particle size region (types B and E). When imaginary components were chosen suitably (types C and F) to reflect the original particle size distribution pattern, the simulated values coincide well with those of the original system. As described before, the simulated values for all the imaginary systems deviate by only a few percent from those of the original system and the measured values.

Some authors have considered the dissolution of polydisperse powders by taking account of the change in particle size distribution with dissolution time[2b,6] and by summing the dissolution behavior of components,[2g] which is similar in principle to the method, based on Eq. 22, *i.e.*, C_T. According to the cube root law (Eqs. 10 and 11), the dissolution behavior is defined by the initial particle size for a monodisperse powder, as can be seen in Figs. 2 and 3. Hence, it was supposed that the dissolution behavior of a polydisperse powder might be predicted when a suitable apparent mean diameter is estimated (Fig. 4). In this paper, even though the particle size range was narrow, the dissolution of mixed sieved particles was examined as model systems of polydisperse powder, and their dissolution processes were well simulated by use of the mean volume diameter, the volume mean diameter and the summation of dissolution behaviors of components whether or not several imaginary components were introduced (Figs. 5, 6 and 9, Tables). Hence, the methods described here might be useful to predict or simulate dissolution processes.

Simulation by the Use of Mean Volume Diameter As described before, dissolution behavior can be well simulated in the terms of mean volume diameter. Hence the usefulness and validity of the mean volume diameter was also examined theoretically for dissolution in a nonsink condition.

Equation 25 is deduced from Eqs. 1 and 4 for a sieved sample.

$$dC=(k/V)n\pi(fD_H)^2\{C_s-(n\pi\rho f^3/6V)(D_{H,\circ}{}^3-D_H{}^3)\}dt \quad (25)$$

Equation 25 can be transformed into Eq. 26 by the use of Eq. 5.

$$-(n\pi\rho/2V)D_H{}^2dD_H=(kn\pi D_H{}^2/V)\{C_s-(n\pi\rho f^3/6V)(D_{H,\circ}{}^3-D_H{}^3)\}dt \quad (26)$$

Rearranging Eq. 26, Eq. 27 is obtained:

$$-dD_H=(2k/\rho)(M_s/V-M_\circ/V+n\pi\rho f^3D_H{}^3/6V)dt \quad (27)$$

where $M_s=C_sV$. In the case of $M_\circ=M_s$ as a nonsink condition, in the same way as Niebergall *et al.* tried to simplify the treatment of dissolution behavior under a nonsink condition,[7] Eq. 27 is simplified to Eq. 28, and Eq. 29 is obtained.

$$-dD_H=(2k/\rho V)(n\pi\rho f^3D_H{}^3/6)dt \quad (28)$$

$$D_H{}^{-2}=D_{H,\circ}{}^{-2}+(4k/\rho V)(n\pi\rho f^3/6)t \quad (29)$$

By multiplying by $(n\pi\rho f^3/6)^{-2/3}$, Eq. 29 is transformed into Eq. 30, and Eq. 31 is obtained for a monodisperse system as a result.

$$M^{-2/3}=M_\circ{}^{-2/3}+(4k/\rho V)(n\pi\rho f^3/6)^{1/3}t \quad (30)$$

$$M^{-2/3}=M_\circ{}^{-2/3}+(4k/\rho V)(M_\circ{}^{1/3}/fD_{H,\circ})t \quad (31)$$

Equation 32 is obtained from Eq. 31 by the use of $w_{i,\circ}$ in place of $M_\circ$ for a mixed system following the approach used to obtain Eq. 16.

$$M^{-2/3}=M_\circ{}^{-2/3}+(4k/\rho Vf)\Sigma(w_{i,\circ}/D_{H,i}{}^3)^{1/3}t \quad (32)$$

Then the following equations are obtained:

$$M^{-2/3}=M_\circ{}^{-2/3}\{1+(4k/\rho Vf)M_\circ{}^{2/3}\Sigma(w_{i,\circ}/D_{H,i}{}^3)^{1/3}t\} \quad (33)$$

$$M^{-2/3}=M_\circ{}^{-2/3}\{1+(4kM_\circ/\rho Vf)M_\circ{}^{-1/3}\Sigma(w_{i,\circ}/D_{H,i}{}^3)^{1/3}t\} \quad (34)$$

$$M^{-2/3}=M_\circ{}^{-2/3}\{1+(4kC_s/\rho fD_v)t\} \quad (35)$$

where $M_\circ/V=M_s/V=C_s$.

Thus, the mean volume diameter is also related to dissolution under a nonsink condition. Therefore, it appears

reasonable to use the mean volume diameter for simulation of dissolution behavior under the conditions described in this paper at least. This conclusion is also thought to be reasonable since the mean volume diameter is given when particle size and weight are given, and the dissolution behavior might be simulated by the use of Eqs. 19 and 35 for a sink condition and a nonsink condition, respectively.

References

1) *a*) H. Sunada, A. Yamamoto, A. Otsuka and Y. Yonezawa, *Chem. Pharm. Bull.*, **36**, 2557 (1988); *b*) H. Sunada, I. Shinohara, A. Otsuka and Y. Yonezawa, *ibid.*, **37**, 467 (1989); *c*) *Idem*, *ibid.*, **37**, 1362 (1989).
2) *a*) D. E. Wurster and J. A. Seitz, *J. Pharm. Sci.*, **49**, 335 (1960); *b*) J. T. Carstensen and M. N. Musa, *ibid.*, **61**, 223 (1972); *c*) P. Pothisiri and J. T. Carstensen, *ibid.*, **63**, 1468 (1973); *d*) M. Partel and J. T. Carstensen, *ibid.*, **64**, 1651 (1975); *e*) J. T. Carstensen and M. Patel, *ibid.*, **64**, 1770 (1975); *f*) I. Matsuura, *Yakugaku Zasshi*, **102**, 264 (1982); *g*) *Idem*, *ibid.*, **102**, 678 (1982).
3) W. Nernst, *Z. Phys. Chem.*, **47**, 52 (1904).
4) A. W. Hixson and J. H. Crowell, *Ind. Eng. Chem.*, **23**, 923 (1931).
5) L. J. Leeson and J. T. Carstensen, "Dissolution Technology," APhA Academy of Pharmaceutical Science, Washington D. C., 1974.
6) W. I. Higchi and E. N. Hiestand, *J. Pharm. Sci.*, **52**, 67 (1963).
7) *a*) P. J. Niebergall and J. E. Goyan, *J. Pharm. Sci.*, **52**, 29 (1963); *b*) P. J. Niebergall, G. Milosovich and J. E. Goyan, *ibid.*, **52**, 236 (1963).